HHS Public Access

Author manuscript

J Bone Miner Res. Author manuscript; available in PMC 2023 February 01.

Published in final edited form as:

J Bone Miner Res. 2022 February ; 37(2): 185–201. doi:10.1002/jbmr.4430.

gp130 cytokines activate novel signaling pathways and alter bone dissemination in ER+ breast cancer cells

Tolu Omokehinde[1,2], **Alec Jotte**[2,3], **Rachelle W. Johnson**[2,4,*]

[1]Graduate Program in Cancer Biology, Vanderbilt University, Nashville, TN, 37232

[2]Vanderbilt Center for Bone Biology, Vanderbilt University Medical Center, Nashville, TN, 37232

[3]Department of Biochemistry, Vanderbilt University, Nashville, TN, 372332

[4]Department of Medicine, Division of Clinical Pharmacology, Vanderbilt University Medical Center, Nashville, TN, 37232

Abstract

Breast cancer cells frequently home to the bone marrow, where they encounter signals that promote survival and quiescence or stimulate their proliferation. The interleukin-6 (IL-6) cytokines signal through the co-receptor glycoprotein130 (gp130) and are abundantly secreted within the bone microenvironment. Breast cancer cell expression of leukemia inhibitory factor (LIF) receptor (LIFR)/STAT3 signaling promotes tumor dormancy in the bone, but it is unclear which, if any of the cytokines that signal through LIFR, including LIF, oncostatin M (OSM), and ciliary neurotrophic factor (CNTF), promote tumor dormancy and which signaling pathways are induced. We first confirmed that LIF, OSM, and CNTF and their receptor components were expressed across a panel of breast cancer cell lines, although expression was lower in estrogen receptor negative bone metastatic clones compared to parental cell lines. In estrogen receptor positive (ER+) cells, OSM robustly stimulated phosphorylation of known gp130 signaling targets STAT3, ERK and AKT, while CNTF activated STAT3 signaling. In ER- breast cancer cells, OSM alone stimulated AKT and ERK signaling. Overexpression of OSM, but not CNTF, reduced dormancy gene expression and increased ER+ breast cancer bone dissemination. Reverse-phase protein array revealed distinct and overlapping pathways stimulated by OSM, LIF, and CNTF with known roles in breast cancer progression and metastasis. In breast cancer patients, downregulation of the cytokines or receptors was associated with reduced relapse-free survival, but OSM was significantly elevated in patients with invasive disease and distant metastasis. Together these data indicate that the gp130 cytokines induce multiple signaling cascades in breast cancer cells, with a potential pro-tumorigenic role for OSM and pro-dormancy role for CNTF.

Introduction

Breast cancer cells frequently metastasize to the bone marrow, which increases patient risk of developing skeletal related events such as fracture, hypercalcemia, and spinal cord compression, and increases mortality [(1,2)]. Upon dissemination into the bone marrow, breast

*Corresponding author: Rachelle W. Johnson, 2215B Garland Ave, 1165C Medical Research Building IV, Nashville, TN 37212, rachelle.johnson@vumc.org.

cancer cells may either induce osteolysis or enter a latent period in which they remain quiescent before emerging as a clinically detectable metastasis [3–5]. While patients with both estrogen receptor positive (ER+) and estrogen receptor negative (ER-) disease develop bone metastases with similar frequency (~50%) [6], the risk of recurrence is different between the two subtypes; in ER- tumors, most skeletal recurrence occurs within the first 5 years after diagnosis, while extended periods of tumor dormancy (8–10 years) prior to skeletal recurrence are more common in ER+ breast cancer [7,8].

One of the signaling molecules identified as a key regulator of tumor dormancy in the bone is leukemia inhibitory factor (LIF) receptor (LIFR) [9], which is also a breast tumor suppressor and metastasis suppressor [10,11]. Breast cancer patients with lower LIFR levels in the primary tumor have significantly worse overall survival [9,11], and breast cancer patients who develop bone metastases have significantly lower LIFR levels in the primary tumor [9]. When LIFR is down-regulated in ER+ breast cancer cells that lie dormant *in vivo*, the tumor cells proliferate and colonize the bone marrow [9]. This is thought to occur through loss of STAT3 signaling, since loss of STAT3 phenocopies tumor cell exit from dormancy in the bone [9] and was previously identified as a pro-dormancy gene in ER+ breast cancer cells [9,12]. LIFR is a member of the interleukin-6 family of cytokines, which induce signaling through the common co-receptor glycoprotein130 (gp130).

There are multiple ligands that form a complex with and initiate downstream signaling through the LIFR/gp130: LIF, oncostatin M (OSM), and ciliary neurotrophic factor (CNTF). LIF and OSM can both form a complex with LIFR/gp130, but OSM can also bind to its cytokine-specific receptor OSM receptor (OSMR). CNTF forms a complex with LIFR/gp130 and its cytokine-specific, soluble receptor CNTF receptor (CNTFR) [13]. While these cytokines are produced in the bone microenvironment [14–18] and are well documented to induce STAT3 signaling in breast cancer cells [9,19–22], it is unclear which, if any, of these cytokines provide signaling cues to induce tumor dormancy. Similarly, while LIF and OSM are known to induce STAT3 signaling [9,19,22–24], MAPK/ERK [23,25–27], and AKT signaling [22,27,28], it is unknown whether these cytokines have differential effects on downstream pathways in breast cancer, and the effect of CNTF on breast cancer cells has not been studied at all.

This study therefore sought to establish the baseline expression of the LIFR-binding cytokines and their receptors in both ER+ and ER- breast cancer cells and their correlation with patient outcomes, identify differentially activated downstream signaling pathways, and determine their effect on tumor growth and dissemination to bone.

Materials and Methods

Cell lines

Human breast cancer cells MCF7 and MDA-MB-231, were acquired from ATCC. Human breast cancer cell line SUM159, were obtained as a gift from the Rutgers Cancer Institute of New Jersey. Bone-tropic MCF7 (MCF7b) were generated in the Johnson Lab and created as previously described [29]. The bone metastatic variant of the MDA-MB-231 cells (MDA-MB-231b) cells were donated to our lab but was previously established as

described [9,30,31]. D2.0R and D2A1 mouse mammary carcinoma cells were donated by the Green laboratory at the National Cancer Institute. Polyoma middle T (PyMT)-derived mouse mammary carcinoma cells were acquired and created by the Anderson laboratory at the Peter MacCallum Cancer Centre. 4T1 mouse mammary carcinoma cells were acquired from ATCC and the bone metastatic variant (4T1BM2) as described [32], were obtained as a gift from the Pouliot laboratory at the Peter MacCallum Cancer Centre.

Cell culture reagents

All cell lines were cultured in DMEM with 10% fetal bovine serum (FBS) and penicillin/streptomycin (P/S) as previously described [9,33]. Human SUM159 breast cancer cells, were cultured in Ham's F12 medium supplemented with 5% FBS, 5 μg mL^{-1} and 1 μg mL^{-1} hydrocortisone.

shRNA Knockdown

Knockdown experiments were performed as previously described [9]. For shRNA experiments 293T cells were transfected with GIPZ lentiviral-LIFR targeting vectors to produce lentivirus. MCF7 cells were transduced with virus using 5 μg mL^{-1} polybrene followed by selection with 1μg/mL puromycin for 3 days.

Stable and Transient Overexpression

MCF7 cells with empty vector and OSM/CNTF overexpression were established by transduction using these expression plasmids: pCMV3-C-GFPSpark Vector (Sino Biologcial, Catalog Number CV026), pCMV3-C-OSM-GFP (Sino Biologcial, Catalog Number HG10452-ACG), pCMV6-AC-GFP (Origene, Catalog Number PS100010) and pCMV6-AC-CNTF-GFP (Origene, Catalog Number RG222331). Cells were selected using hygromycin (OSM) and neomycin (CNTF). MDA-MB-231 parental and bone metastatic cells transiently overexpressing OSM and CNTF were established using previously mentioned expression vectors. Cells were transfected using Lipofectamine LTX with Plus Reagent (Thermo Fisher, Catalog Number 15338030) and harvested 36 hours later.

Real-time PCR

Intact femurs and cells were harvested in TRIzol (Life Technologies), extracted, DNA digested (TURBO DNA-free Kit, Life Technologies), and cDNA synthesized (iScript cDNA Synthesis Kit, Bio-Rad) using the manufacturer's instructions. Real-time PCR was performed using iTaqTM Universal SYBR Green Supermix (Bio-Rad) on a QuantStudio 5 (Thermo Fisher) with the conditions previously described [33]. For each biological replicate, three technical replicates were pipetted onto the qPCR plate and averaged for each gene analyzed. Primers for *B2M, B2m, LIFR, SOCS3*, *THBS1*, *TPM1*, *AMOT*, *TGF-β2*, *P4HA1*, *H2BK*, *IGFBP5*, *miR-190*, and *SBP56* were all previously published [9]. Primers for *QSOX1* [34], *PDCD4* [35], and *CDKN1B* [35] were previously published by other groups. The primer for mouse *gp130* was also previously published [36].

The following primers were designed using PrimerBlast (NCBI) against the human genome (Homo sapiens) and mouse genome (mus musculus) and validated by dissociation: *LIF* F: CCAACGTGACGGACTTCC; *LIF* R: TACACGACTATGCGGTACAGC; *Lif* F:

AACCAGATCAAGAATCAACTGGC; *Lif* R: TGTTAGGCGCACATAGCTTTT; *OSM* F: GGCAGCTGCTCGAAAGAGTA; *OSM* R: ATAGGGGTCCAGGAGTCTGC; *Osm* F: TCATCCTGAGCATGGCACTG: *Osm* R: CGTGAGGTTCGCCTGATTCT: *CNTF* F: GAAGATTCGTTCAGACCTGACTG; *CNTF* R: AAGGTTCTCTTGGAGTCGCTC; *Cntf* F: GCATTTCACCCCGACTGAAG; *Cntf* R: CGCCATTAACTCCTCTAGCTG; *GP130* F: GGAGTGAAGAAGCAAGTGGGA; *GP130* R: AGGCAATGTCTTCCACACGA; *Lifr* F: CTTGCAATGTGCCACTCACT; *Lifr* R: CGAGCACCACTTTGTCTTGA; *OSMR* F: ATGCCATCATGACCTGGAAGG; *OSMR* R: CCTTCACCATGGAGTTCAATCTG; *Osmr* F: AAACATGATATTTCAGATAGAGATCAGTAGACT; *Osmr* R: CTTATGAAATGTTTGACACACTCCAA; *CNTFR* F: TTATGGTCTGTGAGAAGGACCC; *CNTFR* R: GCATTGCTGACACTTATGGAGA; *Cntfr* F: TGTCTACACGCAGAAACACAG; *Cntfr* R: CCCAGACGCTCATACTGCAC; *MSK1* F: TTCCTTTGTTGCTCCTTCCATC; *MSK1* R: CAACATTTGTCACTCCAGGACG; *GATA3* F: GCCCCTCATTAAGCCCAAG; *GATA3* R: TTGTGGTGGTCTGACAGTTCG, *FOXA1* F: GCAATACTCGCCTTACGGCT, *FOXA1* R: TACACACCTTGGTAGTACGCC; *BMP7* F: TCAACCTCGTGGAACATGACA; *BMP7* R: CTTGGAAAGATCAAACCGGAACT; *MAPK14* F: CCCGAGCGTTACCAGAACC; *MAPK14* R: TCGCATGAATGATGGACTGAAAT; *MAPK11* F: AAGCACGAGAACGTCATCGG; *MAPK11* R: TCACCAAGTACACTTCGCTGA; *GAS6* F: GGTAGCTGAGTTTGACTTCCG; *GAS6* R: GACAGCATCCCTGTTGACCTT; *Gapdh* F: AGGTCGGTGTGAACGGATTTG; *Gapdh* R: GGGGTCGTTGATGGCAACA;. For the *in vitro* studies, each target gene was normalized to the expression of the average B2M (human) or *B2m* (mouse) expression within the same sample. For the detection of human cells in mouse samples B2M was normalized to the expression of the average *Gapdh* expression within the same sample.

Recombinant proteins

Recombinant human LIF (R&D Systems), human OSM (R&D Systems), human CNTF (R&D Systems), human CNTFsR (R&D Systems), human IL-6 (R&D Systems), and human IL-6Rα (R&D Systems) were reconstituted in PBS + 0.1% bovine serum albumin (BSA) at 10–50 μg mL^{-1} and aliquoted for storage at −80°C. For all experiments, human recombinant proteins were used on human cell lines. Before cytokine treatment, breast cancer cells were serum starved in DMEM supplemented with 2% FBS overnight and cytokine treatment was made up in fresh media under serum starved conditions.

Reverse Phase Protein Array

MCF7 breast cancer cells were seeded at 1×10^6 cells per dish (Eppendorf) in a 100mm plate cultured overnight. The next day, cells were washed with PBS and plates were reconstituted with DMEM with 2% FBS for serum starvation prior to cytokine treatment as described in the previous section. After 30 minutes of cytokine treatment, cells were washed with PBS and 100μLof RIPA buffer (Sigma) with PhosStop (Phosphatase Inhibitor, Roche, Catalog Number 04–906-845–001) and Protease Inhibitor (Roche/Sigma, Catalog Number 4693159001) and incubated for 30 minutes at 4°C on a plate shaker. Protein concentration was determined by BCA (Thermo Fisher), adjusted to 1.5μg/μL, mixed with (4X SDS and beta-mercaptoethanol) and boiled for 5 minutes. Samples remained at -80°C until sent to

MD Anderson Cancer Center where the samples were processed and analyzed by the RPPA Core facility (analysis included as Supplemental Tables 1–4).

Western Blotting

Cells grown in a monolayer on 100mm cell culture dish were rinsed with 1X PBS and harvested for protein in RIPA buffer supplemented with protease and phosphatase inhibitor. Protein concentration was determined by BCA assay and 18–20μg protein was loaded onto an SDS-PAGE gel and transferred to nitrocellulose membranes using standard techniques. Membranes were probed with antibodies against LIFR (Santa Cruz Biotechnology, C-19, Catalog Number sc-659, 1:1000), pSTAT3 Y705 (Cell Signaling, Catalog Number 9131, 1:1000), STAT3 (Cell Signaling, clone 124H6, Catalog Number 9139, 1:1000), pSTAT1 (Cell Signaling, Catalog Number 9172, 1:1000), STAT1 (Cell Signaling, Catalog Number pAKT Ser473 (Cell Signaling, Catalog Number 9271, 1:1000), AKT (Cell Signaling, Catalog Number 9272S, 1:1000), pERK1/2 Thr202/Tyr204 (Cell Signaling, Catalog Number 9101, 1:1000), ERK1/2 (Cell Signaling, Catalog Number 9102, 1:1000), GAPDH (Cell Signaling, Catalog Number 2118S, 1:1000), alpha-tubulin (Antibody & Protein Resource at Vanderbilt University, Catalog Number VAPRTUB, 1:5000), and vinculin (Millipore, Catalog Number AB6039, 1:10,000). All western blot images were converted to a histogram rendering for each lane and peaks were converted to the relative percentage for each blot. Peaks were quantified as adjusted relative density after the relative percentage for proteins of interest were normalized to the relative percentage of the loading control for the respective lanes. These values were then plotted and defined as relative protein expression. Original, uncropped blots are included as Supplemental Figure 12.

Animals

All experiments were performed in accordance to the guidelines and regulations of the Animal Welfare Act and the Guide for the Care and Use of Laboratory Animals and were approved by the Institutional Animal Care and Use Committee (IACUC) at Vanderbilt University. Experiments were conducted using 4–6-week-old female athymic nude mice (Jackson, Cat #7850). Mice were implanted subcutaneously with 17β-estradiol pellets as described [(29)]. The next day, 1×10^6 tumor cells in 50μL volume of sterile PBS + 50% Matrigel (Fischer Scientific) were injected into the fourth mammary fat pad (n=10 mice/group). Tumor volume was assessed by caliper measurements. Several mice were found dead or had to be sacrificed early due to estrogen toxicities and were removed from the final analysis; all other mice were euthanized 28 days post-inoculation of tumor cells. For the study, final analysis included n=10 MCF7-pCMV3 (Empty Vector) inoculated mice and n=9 MCF7-pCMV3-OSM (OSM overexpression), n=9 MCF7-pCMV6 (Empty Vector) and n=9 MCF7-pCMV6-CNTF (CNTF overexpression).

Flow Cytometry

One hindlimb was crushed with a mortar and pestle to obtain the bone marrow. PBS (1mL) was added to the crushed bone marrow and were spun down and washed with PBS to remove bone debris. Bone marrow (5×10^5 cells) was stained in 100μL of PBS with LIVE/DEAD™ Fixable Green Dead Cell Stain Kit @488nm (Thermo Fisher Scientific, Catalog Number L34970, 1:1000) for 15 minutes on ice at 4°C in the dark. Cells were washed with

PBS and resuspended with 100μL of 1% BSA in PBS with CD298 antibody (BioLegend, Cat #341704) for 30 minutes on ice at 4°C in the dark. Flow cytometry experiments were performed in the VUMC Flow Cytometry Shared Resource using the 5-laser BD LSRII and 4-laser BD Fortessa LSRII. Data was analyzed using FlowJo software (FlowJo, LLC) where bone marrow samples were gated based on forward scatter and side scatter geometry and PE-CD298 (+) cells were gated using live cells (LIVE/DEAD-Green negative). MCF7 breast cancer cells were used as a positive control for CD298 stain.

KM-Plotter and GSE Datasets

KM-Plotter graphs were directly produced using the online bioinformatics tool (https://kmplot.com/) specifically for breast cancer [37].The specific Affymetrix ID for the probes of interest were LIF (205266_at), OSM (214637_at), CNTF (208597_at), LIFR (205876_at), OSMR (205729_at), CNTFR (205723_at), and GP130 (IL6ST-212195_at). Patients were split using the automated best-selection-cutoff analysis provided by the KM-Plotter and median survival between cohorts was computed. No restrictions on analysis were included except for ER status as indicated by microarray [37] in the stratified analysis. A total of n=4929 patients were included in the unstratified analysis and in the ER status analysis, n=3768 ER+ and n=2009 ER- patients were included. The analysis tool has had subsequent updates since its initial creation, culminating to an increase in the number of patients within the database [38,39] and the integration of several tools for more in-depth patient sample analysis [40–43]. Overall, the KM-Plotter total breast cancer patient database includes patient samples from GSE2603, GSE17705, GSE21653, GSE16446, GSE17907 and GSE19615, with a grand total of 7830 patient samples.

For the analysis of the GEO datasets, GSE14548 [44] had a total of 66 samples from fresh-frozen biopsies obtained from the Massachusetts General Hospital. Informed consent was not applicable because specific patient characteristics and data were unavailable to the authors of the study. GSE29044 [45] had a total of 124 samples that were collected from the normal tissue and primary tumors of 109 patients between the ages of 20–62 who underwent treatment and surgery at the King Faisal Specialist Hospital and Research Center of Saudi Arabia. The authors of the study focused on breast cancer patients diagnosed with infiltrating ductal carcinoma (IDC) and ductal carcinoma *in situ* (DCIS). Patient cohorts were stratified by tissue type (normal versus tumor), tumor grade, receptor status, tumor type (IDC versus DCIS) and age. The probes for each cytokine and receptor that were available are listed in Supplemental Table 5 for GSE29044 and in Supplemental Table 6 for GSE14548; we analyzed all of the probes for each sample, and all probes had a similar trend of expression across both GSE datasets. Specific probes were chosen to be displayed in Figure 8, Supplemental Figure 7, 8 and 11 because they are representative of the larger probe set for each gene of interest.

Statistics and reproducibility

For all studies, the scatter dot plots indicate the mean of each group and error bars indicate the standard error of the mean (SEM). All graphs and statistical analyses were generated using Prism software (Graphpad). All *in vitro* assays were performed at least three independent times, and the replicates for each graph contains one replicate from each

independent study. If technical replicates were plated these data were averaged prior to statistical analysis. Data were analyzed for statistical significance using a one-way ANOVA with Dunnett's multiple comparisons test or a two-way ANOVA with Tukey's multiple comparisons test. For *in vitro* assays, no statistical method was used to predetermine sample size. For all analyses $p<0.05$ was considered statistically significant, and *$p<0.05$, **$p<0.01$, ***$p<0.001$, ****$p<0.0001$.

Results

LIFR-binding ligands and receptors are expressed at variable levels in breast cancer cells and reduced in bone metastatic breast cancer

To determine the endogenous expression levels of gp130 cytokines in breast cancer cells, we examined a panel of breast cancer cell lines inclusive of multiple molecular subtypes and species (human and mouse). The human breast cancer cell lines MCF7 (dormant / low metastatic potential *in vivo*, estrogen receptor positive, ER+), SUM159 (dormant / low metastatic potential *in vivo*, estrogen receptor negative, ER-), and MDA-MB-231 (high metastatic potential *in vivo*, ER-) all expressed *LIF*, *OSM* and *CNTF* (Supplemental Figure 1A–C) at variable levels. Similarly, mouse mammary carcinoma cell lines (low metastatic potential: D2.0R and PyMT-derived; high metastatic potential: 4T1 and D2A1) expressed *Lif, Osm*, and *Cntf* (Supplemental Figure 1D–F).

Since all the breast cancer cell lines we examined are able to disseminate to the bone marrow [29–32,46,47], and LIFR is a metastasis suppressor [10] and prevents tumor colonization of bone [9], we examined whether there were differences in cytokine expression between parental and bone-metastatic variants. In comparison to their parental counterparts, there was no significant difference in *LIF* or *CNTF* expression in the bone metastatic variants of the MCF7 cell line (MCF7b) [29] or MDA-MB-231 cells (MDA-MB-231b) [30,31] in comparison to the parental cell lines (Supplemental Figure 1G, I, J, L), but OSM was significantly lower in MDA-MB-231b compared to parental cells (Supplemental Figure 1K; 90%, p=0.0152) and unchanged in MCF7b cells (Supplemental Figure 1H). The bone-metastatic variants for human breast cancer cell line MDA-MB-231 were run concurrently with the parental cell lines, which were re-plotted in Supplemental Figure 1J–L for comparison to the bone metastatic lines. In contrast, *Lif* (82%, p=0.0299), *Osm* (86%, p=0.0271), and *Cntf* (58%, p=0.0076) were all significantly down-regulated in the bone metastatic variant of the 4T1 mouse mammary carcinoma cell line (4T1BM2) [32] compared to the 4T1 parental line (Figure 1A–C). Thus, each breast cancer cell line that was investigated expressed the gp130 ligands at the mRNA level and may therefore be capable of gp130 autocrine signaling.

Since the tumor cell lines expressed the gp130 cytokines, we next examined the endogenous receptor levels across all cell lines to determine whether each component of the LIFR/gp130, OSMR/gp130, and LIFR/CNTFR/gp130 complex is expressed in the breast cancer cells. In the parental human breast cancer cell lines, *GP130*, the co-receptor subunit for not only *LIFR*, *OSMR*, and *CNTFR* but also IL-6 and IL-11 signaling [48–50], was abundantly expressed in MCF7, SUM159, and MDA-MB-231 cells (Supplemental Figure 2A), and *LIFR, OSMR*, and *CNTFR* were all expressed in the human breast cancer cell lines

(Supplemental Figure 2B–D), although *CNTFR* expression was much lower across all cell lines. All the mouse mammary carcinoma cell lines also expressed gp130 and the cytokine specific receptors, again with particularly low CNTFR expression across all cell lines (Supplemental Figure 2E–H).

Upon examination of the bone-metastatic cell lines, MCF7b cells had no significant change in *GP130, LIFR*, *OSMR*, or *CNTFR* (Supplemental Figure 2I–L), nor did MDA-MB-231b cells compared to the parental cell line (Supplemental Figure 2M–P). In 4T1BM2 cells, *gp130* was unchanged (Supplemental Figure 2Q), but *Lifr* (85%, p=0.0081), *Osmr* (73%, p=0.0344), and *Cntfr* (82%, p=0.0036) were all significantly reduced (Figure 1D–F). Thus, all of the receptors required for LIFR signaling are expressed in breast cancer cell lines, although some of the receptors are expressed at lower levels in bone-metastatic cells.

We next examined whether patterns of expression for the cytokines or receptors aligned with ER status. Upon clustering expression values from Figure 1 and Supplemental Figures 1 and 2 into ER+ and ER- cell lines, there was no significant change in the expression of *LIF, OSM, CNTF* or *GP130* (Supplemental Figure 3A–D) between ER+ and ER- human breast cancer cell lines. In contrast, the cytokine specific receptors *LIFR* (66%, p=0.0224)*, OSMR* (64%, p<0.0001) *and CNTFR* (96%, p=0.0006) were all significantly reduced in the human ER- breast cancer cell lines when compared to the ER+ cell lines (Supplemental Figure 3E–G). In mouse cell lines, *Cntf* (44%, p=0.0207) and *Lifr* (85%, p=0.0390) were significantly lower in ER- compared to ER+ cell lines, with no significant changes in *Lif*, *Osm*, *gp130*, *Osmr*, or *Cntfr* (Supplemental Figure 3H–N).

The expression of gp130, LIFR, OSMR, and CNTFR in breast cancer cells suggests that breast cancer cells possess all of the machinery to induce downstream signaling in response to both autocrine and paracrine-secreted gp130 ligands. Breast cancer cells have been shown to colonize the osteogenic niche, and it was previously reported that osteoblast lineage cells express LIF [16,18], OSM [17], and CNTF [14,15], along with hematopoietic cell lineages and stromal cells [51] suggesting that bone-disseminated tumor cells in the osteogenic niche may be exposed to these signals. We have confirmed that these cytokines are also expressed at the transcript level in homogenized mouse femora, which include bone marrow (Supplemental Figure 3O).

OSM activates STAT3, ERK, and AKT signaling in MCF7 cells

Since breast cancer cells express the necessary signal transduction machinery for LIFR signaling, we next examined whether the cytokines induce known gp130 downstream signaling pathways. LIF, OSM, and CNTF have all been previously reported to activate AKT, ERK, and STAT signaling [9,19–23,25–28,52,53], but the relative induction of these downstream signaling pathways, and in response to CNTF in particular, has not been explored in breast cancer. While the MCF7 cells have low basal phosphorylated AKT (pAKT) and ERK (pERK), OSM dramatically activated AKT (up to a 9-fold increase, p<0.0001) and ERK (up to a 5-fold increase, p=0.0542–0.0001) signaling, while LIF only activated ERK signaling (up to a 3-fold increase, p=0.0025) above baseline (Figure 2A–C). CNTF alone did not activate either pathway, as indicated by pAKT and pERK expression, but modestly increased ERK signaling (p=0.0130) when combined with its

soluble receptor CNTFR (sR), which has been reported to mediate downstream CNTF signaling in osteoblasts [14]. In contrast, LIF, OSM, and CNTF all robustly activated the STAT3 signaling pathway, as indicated by up to a 37-fold increase in phosphorylated STAT3 ($pSTAT3^{Y705}$) when compared to PBS control (Figure 2A, D; p=0.0001 – 0.0017). CNTF and CNTF+sR (CNTFsR) activation of STAT3 signaling was only significant at 15 minutes (Figure 2D), but still induced pSTAT3 signaling well above baseline at 30 minutes (Figure 2A). Thus, OSM is the most potent signal transducer of AKT, ERK, and STAT3 signaling in ER+ breast cancer cells.

OSM activates STAT3 and AKT signaling in MDA-MB-231b cells

We and others have previously reported that MDA-MB-231 and MDA-MB-231b cells express LIFR at the protein level, but that it is non-functional, since treatment with LIF does not activate downstream STAT3 signaling [9,20]. While OSM activated AKT in MDA-MB-231 cells, with up to a 4-fold increase in pAKT, neither LIF, CNTF nor CNTF/CNTFsR treatment induced pAKT (Figure 2E, F; p=0.0101 – 0.0227). Since MDA-MB-231 cells have constitutive ERK activation [26], we saw no further enhancement of ERK signaling by any of the ligands (Figure 2E, G). As previously demonstrated, recombinant LIF did not activate STAT3 signaling, while OSM dramatically activated STAT3 signaling (Figure 2E, H; up to 2.41-fold increase, p<0.0001). MDA-MB-231b cells were unresponsive to CNTF and CNTFsR (Figure 2E–H), consistent with the need for a functional LIFR, which both the MDA-MB-231 and MDA-MB-231b cells lack [9,20]. Despite LIFR being non-functional in the MDA-MB-231b cells, OSM was still able to activate STAT3 signaling, suggesting that OSM specifically may still be able to induce downstream signaling through LIFR in breast cancer cells, or that OSM may be able to signal through the OSMR, which was expressed in both MDA-MB-231 and MDA-MB-231b cells (Supplemental Figure 2O). Collectively these data indicate that OSM is the most potent inducer of downstream signaling in ER- and ER+ breast cancer cells.

LIFR is required for LIF but not OSM induction of downstream signaling

Given that MCF7 cells express both OSMR and LIFR, we next aimed to determine whether MCF7 cells retain their responsivity to OSM and LIF when LIFR is knocked down. When compared to MCF7 non-silencing control (NSC) cells, two distinct MCF7 shLIFR cell lines (generated from pooled populations of two different shRNAs) had reduced expression of LIFR (Supplemental Figure 4A–C), as expected. It is important to note that while each cell line is represented by its own blot, all blots were developed simultaneously for NSC and shLIFR cell lines at 15 and 30 minutes. LIF (78–89% increase, p=0.0005 – 0.0039), OSM (81–90% increase, p<0.0001 – 0.0013) and IL-6 (75–86% increase, p=0.0021 – 0.0401), which was included as a control since it does not require LIFR to signal, significantly activated STAT3 signaling in MCF7 NSC cells as indicated by pSTAT3 (Y705) levels (Supplemental Figure 4A, D, E). However, in MCF7 shLIFR cells, LIF activation of STAT3 signaling was no longer significant (Supplemental Figure 4D, E). LIF activation of AKT and ERK was similarly dampened in the MCF7 shLIFR cells (Supplemental Figure 4A–C, F–I). In contrast, OSM robustly activated STAT3 and AKT signaling up to a 72-fold increase, regardless of LIFR knockdown (Supplemental Figure 4A–I; p=0.0001 – 0.0055). OSM induction of ERK was significantly dampened with LIFR knockdown (Supplemental Figure

4A–C, H; p=0.2290 – 0.8960). As expected and similar to IL-6 activation of STAT3, IL-6 stimulation resulted in an increase in AKT (83–95% increase) and ERK (37%-93% increase) activation when compared to the PBS control, regardless of LIFR knockdown (Supplemental Figure 4A–C, F–I). OSM therefore remains a potent inducer of downstream signaling even when LIFR expression is reduced.

OSM promotes spontaneous dissemination of MCF7 cells to the bone

To determine whether autocrine gp130 signaling alters tumor progression and known dormancy-promoting genes [9], we constitutively over-expressed OSM, LIF, and CNTF in MCF7 cells. We chose the MCF7 model for these experiments since they are ER+ and patients with ER+ disease typically have much longer latency (dormancy) periods prior to recurrence than patients with ER- disease (5–10 years compared to <5 years) [6,7], and patients with ER+ breast cancers are also more likely to develop bone-only metastases [54]. We and others have also published that MCF7 tumor cells remain dormant in distant sites including the lung and bone marrow following inoculation [9,29,33,47,55]. The OSM and CNTF overexpression plasmids had unique plasmid backbones (OSM: pCMV3, CNTF: pCMV6) and were each compared to their respective control cell lines expressing the empty vector. We were unable to generate stable LIF overexpressing cells (data not shown), which we hypothesize may be due to dormancy induction within the LIF-overexpressing clones. Overexpression of OSM and CNTF was confirmed by qPCR (Supplemental Figure 5A, B; 107-fold - p<0.0079, 4000-fold - p<0.0003) in MCF7 cells (OSM-OE and CNTF-OE). Utilizing these overexpression cells, we sought to determine the role of OSM and CNTF in primary tumor growth *in vivo*, OSM-OE and CNTF-OE or control MCF7 cells were inoculated into the mammary fat pad of mice with estradiol supplementation (n=10 mice/group). Over-expressing cells were re-validated for OSM and CNTF overexpression at the time of inoculation (data not shown). Overexpression of OSM resulted in a modest but significant increase in primary tumor volume at end point with a trend toward an increase in tumor weight (Figure 3A&B). We also examined whether tumor dissemination to bone was impacted by OSM overexpression, using previously published techniques to detect ultra-low levels of bone-disseminated tumor cells [33]. Assessment of tumor burden by qPCR for the human housekeeping gene *B2M* did not yield any detectable expression in the femurs of mice inoculated with either empty vector or OSM-overexpressing cells (Figure 3C) but more sensitive flow cytometric analysis of bone-disseminated CD298+ tumor cells [33] revealed a significant increase in the number and percentage of CD298+ tumor cells in the bone in mice inoculated with OSM-overexpressing tumor cells, regardless of whether tumor burden was normalized to primary tumor weight at sacrifice (Figure 3D–G; p=0.0009 – 0.0401). Overexpression of CNTF did not significantly alter primary tumor volume but modestly increased primary tumor weight at the endpoint of the study (Supplemental Figure 5E, F). There was no change in bone-disseminated tumor burden in mice inoculated with CNTF-overexpressing tumor cells by either qPCR or flow cytometric analysis, regardless of whether the data were normalized to primary tumor weight (Supplemental Figure 5G–K). Of note, a slight trend in increased bone dissemination in CNTF overexpressing cells was observed; however, this effect was reversed when normalized to final tumor weight (Supplemental Figure 5H&J). Thus, OSM, but not CNTF promotes ER+ tumor dissemination to bone.

Constitutive expression of OSM, but not CNTF, reduces pro-dormancy genes in ER+ breast cancer cells

To determine whether the OSM-induced increase in bone-disseminated tumor cells may be due to cells exiting dormancy, we examined expression of pro-dormancy genes in OSM and CNTF-overexpressing cells. Overexpression of OSM in MCF7 cells (OSM-OE) significantly reduced the expression of 6/21 pro-dormancy genes [9], including *MAPK11* (p38β), *BMP7*, *FOXA1*, *IGFBP5*, *PDCD4*, and *TGFB2* when compared to the empty vector expressing control cell line (Figure 4A; 41–97.5%, $p<0.05$–0.0001). In contrast, one gene, *BMP7*, was significantly reduced in CNTF-over-expressing MCF7 (CNTF-OE) cells (Figure 4B; 20%, $p=0.0223$). Using the same expression vectors, we transiently over-expressed OSM and CNTF in MDA-MB-231 parental and bone-metastatic cells to determine if gp130 signaling alters dormancy related genes in ER- breast cancer cell lines. Overexpression of OSM (2500-fold, $p=0.0188$) in MDA-MB-231 parental cells significantly reduced *GAS6* expression ($p=0.0064$; Supplemental Figure 6A&C); CNTF overexpression (2400-fold, $p=0.0100$) did not alter any of the dormancy genes (Supplemental Figure 6B&D). Overexpression of OSM (32,000-fold) in MDA-MB-231b cells significantly increased *SOCS3* ($p=0.0417$) and *MAPK11* (p38β, $p=0.0211$) (Figure 4C, Supplemental Figure 5C), but CNTF overexpression (626-fold, $p=0.0122$) had no effect on any dormancy genes (Figure 4D, Supplemental Figure 5D). It is therefore possible that OSM reduces pro-dormancy genes to promote the outgrowth of tumor cells in the bone.

The gp130 cytokines activate novel signaling pathways in breast cancer cells

Previous studies have demonstrated that loss of LIFR in ER+ MCF7 cells leads to tumor outgrowth in the bone [9], but our data indicates that OSM is the most potent signal transducer and promotes tumor dissemination while repressing dormancy. To further understand how OSM may be acting as a pro-metastatic factor, we examined the complex downstream signaling activated by the gp130 cytokines by performing molecular reverse phase protein array (RPPA) profiling of MCF7 cells treated with recombinant LIF, OSM, CNTF or CNTF+sR (50ng/ml) for 15 minutes. Of the 496 phospho-specific and total antibodies tested, 38 proteins were significantly altered in the presence of one of the gp130 cytokines compared to PBS controls. Our findings highlight the cascade of signaling pathways activated by the GP130 cytokines *LIF*, *OSM*, *CNTF*, *CNTF:CNTF+sR* and the interconnectivity between the downstream signaling proteins in ER+ breast cancer cells (Figure 5A–F, Supplemental Figure 6E–G). We also analyzed the relative induction of downstream signaling pathways by one-way ANOVA with multiple comparisons, which yielded 13 protein targets (Supplemental Figure 6H). OSM specifically activated major downstream mediators of the AKT, STAT, and ERK signaling pathways (Figure 6A–D), consistent with our findings in Figure 2, as well as mediators of the mTOR, HSP27, and Src signaling pathways (Figure 6E–H). LIF also stimulated the Src signaling pathway (Figure 6H, 7A), while CNTF activated mTOR (Figure 6F), Src (Figure 6H) and MTCO1 (Figure 7B) downstream signaling. Interestingly, there were several pathways that were negatively regulated by the addition of sCNTFR, including MTCO1, NRAS, PREX1, and PYGB (Figure 7B–E). Of note, Src signaling was activated by all three cytokines both in the one-way ANOVA and by the individual cytokine analysis, suggesting this is a key signaling pathway activated downstream of gp130 in breast cancer. We therefore examined

Src expression and several downstream signaling targets in the GSE14548 (Supplemental Figure 7) and GSE29044 (Supplemental Figure 8) datasets. Not all targets were available for both datasets; however, in both datasets, *c-SRC* and *KRAS* were significantly increased in invasive tumors. p190RhoGAP and NRAS were also significantly increased in the GSE14548 dataset. Interestingly, p38α (*MAPK14*) was significantly elevated in both datasets in the invasive tumors, and STAT3 was increased in GSE14548, both pro-dormancy factors [9,12] that are downstream of Src signaling [56–59]

Expression of the gp130 cytokines and receptors is associated with increased survival in breast cancer patients

Lastly, we examined whether the expression of these cytokines and receptors were associated with clinical outcomes in breast cancer patients. Kaplan Meier (KM) Plotter analysis revealed that relapse-free survival (RFS) was significantly reduced in all breast cancer patients with lower expression levels of the gp130 ligands or receptors, including OSM and OSMR, (Supplemental Figure 9; $p<0.0001$), regardless of whether patients had ER+ or ER- tumors (Supplemental Figure 10; $p<0.0001$). Analysis from two additional independent datasets (GSE14548 and GSE29044 [29]) demonstrated that *LIFR* mRNA expression, but not *LIF*, was significantly reduced in patients with both non-invasive ductal carcinoma *in situ* (DCIS) and invasive ductal carcinoma (IDC) (Figure 8A–B, Supplemental Figure 11A–B; $p<0.0001 – 0.0085$). OSMR expression was unchanged in DCIS and IDC patient samples in the GSE29044 dataset (Supplemental Figure 11C), but OSM was increased in the GSE29044 dataset (Supplemental Figure 11D), and OSM and OSMR were significantly increased in DCIS and invasive carcinoma in the GSE14548 dataset (Figure 8C, D; $p=0.0006 – 0.0216$). gp130 expression was also reduced in patients with IDC (Figure 8E; $p=0.0337$) from the GSE29044 data set, but not in the GSE14548 dataset (Supplemental Figure 11E). CNTF and CNTFR levels were unchanged with breast cancer stage (Figure 8F, G and Supplemental Figure 11F); CNTF was not included in the GSE29044 dataset.

Discussion

This study explores and characterizes the function of the gp130 cytokines in several breast cancer cell lines and patient datasets by highlighting the relative expression of the ligands and cytokine specific receptors, identifying novel signaling pathways activated by the cytokine family, and assessing the *in vivo* outcomes of breast cancer bone colonization (Figure 8H). We utilized a panel of breast cancer cell lines with varying molecular characteristics to assess the expression of the gp130 cytokines across multiple subtypes, including highly metastatic cell lines (e.g. MDA-MB-231, 4T1) and cell lines that are considered dormant (e.g. MCF7, D2.0R), given the lack of growth and colonization of distant metastatic sites following inoculation [9,12,47,60]. Our data indicate that all of the cytokines and receptors that are required for autocrine or paracrine OSM, LIF, and CNTF signaling are present in all breast cancer subtypes at the transcript level; however, we can conclude that expression of the receptors (LIFR, OSMR, CNTFR, and gp130) is considerably lower in ER- compared to ER+ disease, suggesting that loss of the gp130-related receptors (not just LIFR, as we previously reported), may be associated with more aggressive disease. These data are consistent with our previously published work

demonstrating that LIFR signaling is lower across cells with high metastatic potential [9], which tend to be ER-.

OSM has been shown to induce metastatic characteristics of ER+ breast cancer cells [61], and is associated with EMT and the detachment of tumor cells [62]. In 4T1 triple negative breast cancer (TNBC) cells, (which lack ER, progesterone receptor/PR, and HER2), OSM knockdown reduces osteolytic bone destruction and spontaneous metastasis to the spine [63]. Our study suggests that OSM also promotes dissemination of ER- cells to the bone, but loss of OSM signaling may increase proliferation of bone-disseminated tumor cells, as evidenced by lower DMFS and the lower expression of OSM we observed in the bone metastatic clones of both TNBC breast cancer cell lines. While the mechanism by which OSM downregulation promotes tumor outgrowth remains unknown, OSM increased SOCS3 and p38 signaling specifically in the bone-metastatic MDA-MB-231 cells, suggesting loss of these signaling pathways as potential mechanisms to explore. Our data also suggests there may be an inverse correlation between OSM expression in the primary tumor and bone metastases in patients with TNBC.

In ER+ breast cancer, our data indicate a pattern similar to ER- breast cancer: OSM drives bone dissemination, but loss of OSM promotes tumor outgrowth in the bone. However, our data indicate that OSM may be downregulated more frequently in ER- compared to ER+ breast cancer. Thus, while OSM drives dissemination to bone and reduces pro-dormancy genes in ER+ breast cancer, our data indicate that ER+ breast cancer cells frequently retain OSM expression and remain dormant in the bone.

The question therefore remains how OSM and LIFR signal together to regulate tumor progression and dormancy. OSM is a ligand for the LIFR, which acts as a tumor suppressor [10,11] and pro-dormancy factor in bone [9], and OSM appears to be the most potent signal transducer of all the gp130 cytokines in breast cancer cells. However, OSM promotes bone dissemination and activates multiple pro-tumorigenic signaling pathways. How, then, does LIFR suppress tumor progression and emergence from dormancy with OSM inducing these pro-tumorigenic signaling pathways? The clinical data suggest that OSM expression is beneficial for long-term patient outcomes. Of note, OSM robustly induces ERK, AKT, and STAT3 signaling, and STAT3 is a part of an ER+ dormancy signature [12] and promotes dormancy of ER+ breast cancer cells in the bone [9]. Thus, OSM induction of STAT3 may be the dominant signaling pathway in ER+ tumor cells once they have disseminated to bone. In the primary tumor, as in our model reported here, the balance may be tipped toward ERK and AKT or the other pro-tumorigenic pathways we identified, with suppression of pro-dormancy genes helping to fuel tumor proliferation. It also cannot be ruled out that our *in vivo* findings may be impacted by the immunodeficient mouse model or estradiol treatment that is required for ER+ xenograft models. Follow-up studies in syngeneic models will shed light on this, but it is important to note that our studies are consistent with previous findings that OSM promotes bone colonization in a syngeneic immunocompetent mouse model [63].

Our findings demonstrate that LIF, OSM, and CNTF all robustly phosphorylate Src (Y527), but the significance of this is unclear given that the three cytokines do not appear to have

the same effect on tumor dissemination to bone (OSM promotes, CNTF has no effect, and LIF is unknown). Despite being in a 'closed' confirmation [64–66], Src^{Y527} overexpression in MDA-MB-231 breast cancer cells results in increased bone and lung dissemination, and osteolytic bone destruction [67]. In patient studies, high Src^{Y527} expression is significantly associated with metastatic disease, poor progression-free survival, and significantly worse bone metastasis-free survival [68,69]. This suggests that OSM in particular may promote metastasis through activation of a Src^{Y527} signaling axis; however, given that the pro-dormancy factor p38α and STAT3 expression were elevated in invasive disease alongside Src signaling factors, further studies will be necessary to determine the role for Src signaling downstream of the gp130 cytokines in breast cancer progression and metastasis.

While there are multiple reports of OSM promoting tumor proliferation and bone metastasis [21,61–63,70], there is relatively little known about the role for OSMR in bone metastasis. OSM can form a complex with either LIFR/gp130 or OSMR/gp130 [52], and therefore the effects of OSM and activation of downstream signaling pathways such as STAT3, ERK, AKT, and Src signaling in breast cancer cells may be mediated through either LIFR or OSMR, but previous studies have not determined which receptor is responsible. Our data from shLIFR knockdown cells suggest that OSM may activate STAT3 and AKT signaling through the OSMR, but activates ERK signaling through both the LIFR and OSMR; however, LIFR knockdown was incomplete in our model and OSM may therefore continue to signal through residual LIFR. Indeed, LIF modestly induced STAT3 signaling in shLIFR cells, and although this did not reach statistical significance, it suggests some active, residual LIFR persists. Future studies examining the role for OSMR in tumor progression and whether it is required for OSM induction of downstream signaling will be of interest.

CNTF has been widely studied for its role in the nervous system and neurite outgrowth [71] and effects on bone formation [14,15]. The data presented here is the first to report the effects of CNTF on breast cancer signaling and tumor progression and suggest that CNTF may prevent tumor progression and bone metastasis in patients with ER- but not ER+ disease. However, we cannot rule out potential effects of CNTF on later stages of metastatic progression in ER+ disease, such as regulation of bone colonization by disseminated tumor cells. Since CNTF preferentially activates STAT3 over AKT or ERK signaling in ER+ cells, and we previously reported that STAT3 induces dormancy in the bone [9], this suggests that CNTF may be the most likely of the three cytokines to induce dormancy. This may also point to a potential role for CNTF/CNTFR in preventing colonization of bone in more aggressive or later stages of bone metastatic disease.

In conclusion, the gp130 cytokines play a nuanced role in tumor progression and bone dissemination and activate multiple signaling pathways in breast cancer cells. Our findings also suggest a potential stimulatory role for OSM in ER+ breast cancer bone dissemination and a potential inhibitory effect of CNTF on bone metastasis in ER- breast cancer and emergence from dormancy in ER+ breast cancer. Continued study of these signaling pathways in breast cancer may uncover novel ways to prevent tumor progression and the formation of bone metastases.

Supplementary Material

Refer to Web version on PubMed Central for supplementary material.

Acknowledgements

T.O. is supported by an HHMI Gilliam Fellowship. R.W.J. is supported by NIH award R00CA194198 (R.W.J.) and DoD Breakthrough Award W81XWH-18-1-0029 (R.W.J.). This project was also supported by scholarship funds from NIH award P30CA068485 Vanderbilt-Ingram Cancer Center Support Grant. The authors have nothing to disclose.

References

1. Kuchuk I, Hutton B, Moretto P, Ng T, Addison CL, Clemons M. Incidence, consequences and treatment of bone metastases in breast cancer patients—Experience from a single cancer centre. Journal of Bone Oncology. 2013/12/01/ 2013;2(4):137–44. [PubMed: 26909284]
2. Coleman RE. Metastatic bone disease: clinical features, pathophysiology and treatment strategies. Cancer Treatment Reviews. 2001/06/01/ 2001;27(3):165–76. [PubMed: 11417967]
3. Sterling JA, Guelcher SA. Bone structural components regulating sites of tumor metastasis. Current osteoporosis reports. Jun 2011;9(2):89–95.
4. Croucher PI, McDonald MM, Martin TJ. Bone metastasis: the importance of the neighbourhood. Nat Rev Cancer. May 25 2016;16(6):373–86. Epub 2016/05/26. [PubMed: 27220481]
5. Salvador F, Llorente A, Gomis RR. From latency to overt bone metastasis in breast cancer: potential for treatment and prevention. The Journal of pathology. Sep 2019;249(1):6–18. Epub 2019/05/17. [PubMed: 31095738]
6. Han HH, Lee SH, Kim BG, Lee JH, Kang S, Cho NH. Estrogen Receptor Status Predicts Late-Onset Skeletal Recurrence in Breast Cancer Patients. Medicine. Feb 2016;95(8):e2909. Epub 2016/03/05. [PubMed: 26937933]
7. Savci-Heijink CD, Halfwerk H, Hooijer GK, Horlings HM, Wesseling J, van de Vijver MJ. Retrospective analysis of metastatic behaviour of breast cancer subtypes. Breast cancer research and treatment. Apr 2015;150(3):547–57. Epub 2015/03/31. [PubMed: 25820592]
8. Wei B, Wang J, Bourne P, Yang Q, Hicks D, Bu H, et al. Bone metastasis is strongly associated with estrogen receptor-positive/progesterone receptor-negative breast carcinomas. Human pathology. Dec 2008;39(12):1809–15. Epub 2008/08/22. [PubMed: 18715613]
9. Johnson RW, Finger EC, Olcina MM, Vilalta M, Aguilera T, Miao Y, et al. Induction of LIFR confers a dormancy phenotype in breast cancer cells disseminated to the bone marrow. Nat Cell Biol. Oct 2016;18(10):1078–89. Epub 2016/09/20. [PubMed: 27642788]
10. Chen D, Sun Y, Wei Y, Zhang P, Rezaeian AH, Teruya-Feldstein J, et al. LIFR is a breast cancer metastasis suppressor upstream of the Hippo-YAP pathway and a prognostic marker. Nature medicine. Oct 2012;18(10):1511–7.
11. Iorns E, Ward TM, Dean S, Jegg A, Thomas D, Murugaesu N, et al. Whole genome in vivo RNAi screening identifies the leukemia inhibitory factor receptor as a novel breast tumor suppressor. Breast cancer research and treatment. Aug 2012;135(1):79–91. [PubMed: 22535017]
12. Kim RS, Avivar-Valderas A, Estrada Y, Bragado P, Sosa MS, Aguirre-Ghiso JA, et al. Dormancy signatures and metastasis in estrogen receptor positive and negative breast cancer. PLoS One. 2012;7(4):e35569. Epub 2012/04/25. [PubMed: 22530051]
13. Davis S, Aldrich TH, Stahl N, Pan L, Taga T, Kishimoto T, et al. LIFR beta and gp130 as heterodimerizing signal transducers of the tripartite CNTF receptor. Science (New York, NY). Jun 18 1993;260(5115):1805–8. Epub 1993/06/18.
14. McGregor NE, Poulton IJ, Walker EC, Pompolo S, Quinn JM, Martin TJ, et al. Ciliary neurotrophic factor inhibits bone formation and plays a sex-specific role in bone growth and remodeling. Calcified tissue international. Mar 2010;86(3):261–70. Epub 2010/02/17. [PubMed: 20157807]

15. Liu F, Aubin JE, Malaval L. Expression of leukemia inhibitory factor (LIF)/interleukin-6 family cytokines and receptors during in vitro osteogenesis: differential regulation by dexamethasone and LIF. Bone. Jul 2002;31(1):212–9. Epub 2002/07/12. [PubMed: 12110437]

16. Ishimi Y, Abe E, Jin CH, Miyaura C, Hong MH, Oshida M, et al. Leukemia inhibitory factor/differentiation-stimulating factor (LIF/D-factor): regulation of its production and possible roles in bone metabolism. Journal of cellular physiology. Jul 1992;152(1):71–8. [PubMed: 1618924]

17. Walker EC, McGregor NE, Poulton IJ, Solano M, Pompolo S, Fernandes TJ, et al. Oncostatin M promotes bone formation independently of resorption when signaling through leukemia inhibitory factor receptor in mice. J Clin Invest. Feb 2010;120(2):582–92. Epub 2010/01/07. [PubMed: 20051625]

18. Allan EH, Hilton DJ, Brown MA, Evely RS, Yumita S, Metcalf D, et al. Osteoblasts display receptors for and responses to leukemia-inhibitory factor. J Cell Physiol. Oct 1990;145(1):110–9. Epub 1990/10/01. [PubMed: 2170427]

19. Lapeire L, Hendrix A, Lambein K, Van Bockstal M, Braems G, Van Den Broecke R, et al. Cancer-associated adipose tissue promotes breast cancer progression by paracrine oncostatin M and Jak/STAT3 signaling. Cancer Res. Dec 1 2014;74(23):6806–19. Epub 2014/09/26. [PubMed: 25252914]

20. Zeng H, Qu J, Jin N, Xu J, Lin C, Chen Y, et al. Feedback Activation of Leukemia Inhibitory Factor Receptor Limits Response to Histone Deacetylase Inhibitors in Breast Cancer. Cancer Cell. Sep 12 2016;30(3):459–73. Epub 2016/09/14. [PubMed: 27622335]

21. Tawara K, Scott H, Emathinger J, Wolf C, LaJoie D, Hedeen D, et al. HIGH expression of OSM and IL-6 are associated with decreased breast cancer survival: synergistic induction of IL-6 secretion by OSM and IL-1β. Oncotarget. Mar 12 2019;10(21):2068–85. Epub 2019/04/23. [PubMed: 31007849]

22. Junk DJ, Bryson BL, Smigiel JM, Parameswaran N, Bartel CA, Jackson MW. Oncostatin M promotes cancer cell plasticity through cooperative STAT3-SMAD3 signaling. Oncogene. 2017;36(28):4001–13. Epub 2017/03/13. [PubMed: 28288136]

23. Stahl N, Boulton TG, Farruggella T, Ip NY, Davis S, Witthuhn BA, et al. Association and activation of Jak-Tyk kinases by CNTF-LIF-OSM-IL-6 beta receptor components. Science (New York, NY). Jan 7 1994;263(5143):92–5. Epub 1994/01/07.

24. Matsuda T, Nakamura T, Nakao K, Arai T, Katsuki M, Heike T, et al. STAT3 activation is sufficient to maintain an undifferentiated state of mouse embryonic stem cells. Embo j. Aug 2 1999;18(15):4261–9. Epub 1999/08/03. [PubMed: 10428964]

25. Takahashi-Tezuka M, Yoshida Y, Fukada T, Ohtani T, Yamanaka Y, Nishida K, et al. Gab1 acts as an adapter molecule linking the cytokine receptor gp130 to ERK mitogen-activated protein kinase. Molecular and cellular biology. Jul 1998;18(7):4109–17. Epub 1998/06/25. [PubMed: 9632795]

26. Li C, Ahlborn TE, Kraemer FB, Liu J. Oncostatin M-induced growth inhibition and morphological changes of MDA-MB231 breast cancer cells are abolished by blocking the MEK/ERK signaling pathway. Breast cancer research and treatment. Mar 2001;66(2):111–21. Epub 2001/07/05. [PubMed: 11437097]

27. Fahmi A, Smart N, Punn A, Jabr R, Marber M, Heads R. p42/p44-MAPK and PI3K are sufficient for IL-6 family cytokines/gp130 to signal to hypertrophy and survival in cardiomyocytes in the absence of JAK/STAT activation. Cellular signalling. Apr 2013;25(4):898–909. Epub 2012/12/27. [PubMed: 23268184]

28. Li X, Yang Q, Yu H, Wu L, Zhao Y, Zhang C, et al. LIF promotes tumorigenesis and metastasis of breast cancer through the AKT-mTOR pathway. Oncotarget. Feb 15 2014;5(3):788–801. Epub 2014/02/21. [PubMed: 24553191]

29. Clements ME, Johnson RW. PREX1 drives spontaneous bone dissemination of ER+ breast cancer cells. Oncogene. Feb 2020;39(6):1318–34. Epub 2019/10/23.

30. Guise TA, Yin JJ, Taylor SD, Kumagai Y, Dallas M, Boyce BF, et al. Evidence for a causal role of parathyroid hormone-related protein in the pathogenesis of human breast cancer-mediated osteolysis. The Journal of clinical investigation. Oct 1 1996;98(7):1544–9. [PubMed: 8833902]

31. Johnson RW, Nguyen MP, Padalecki SS, Grubbs BG, Merkel AR, Oyajobi BO, et al. TGF-beta promotion of Gli2-induced expression of parathyroid hormone-related protein, an important

osteolytic factor in bone metastasis, is independent of canonical Hedgehog signaling. Cancer Res. Feb 1 2011;71(3):822–31. Epub 2010/12/30. [PubMed: 21189326]

32. Kusuma N, Denoyer D, Eble JA, Redvers RP, Parker BS, Pelzer R, et al. Integrin-dependent response to laminin-511 regulates breast tumor cell invasion and metastasis. International journal of cancer Journal international du cancer. Feb 1 2012;130(3):555–66. [PubMed: 21387294]
33. Sowder ME, Johnson RW. Enrichment and detection of bone disseminated tumor cells in models of low tumor burden. Scientific Reports. 2018/09/24 2018;8(1):14299. [PubMed: 30250146]
34. Poillet L, Pernodet N, Boyer-Guittaut M, Adami P, Borg C, Jouvenot M, et al. QSOX1 inhibits autophagic flux in breast cancer cells. PLoS One. 2014;9(1):e86641. Epub 2014/01/30. [PubMed: 24475161]
35. Oki T, Nishimura K, Kitaura J, Togami K, Maehara A, Izawa K, et al. A novel cell-cycle-indicator, mVenus-p27K-, identifies quiescent cells and visualizes G0-G1 transition. Sci Rep. Feb 6 2014;4:4012. Epub 2014/02/07. [PubMed: 24500246]
36. Johnson RW, Brennan HJ, Vrahnas C, Poulton IJ, McGregor NE, Standal T, et al. The Primary Function of gp130 Signaling in Osteoblasts Is To Maintain Bone Formation and Strength, Rather Than Promote Osteoclast Formation. Journal of Bone and Mineral Research. 10.1002/jbmr.2159 2014/06/01 2014;29(6):1492–505. [PubMed: 24339143]
37. Győrffy B, Lanczky A, Eklund AC, Denkert C, Budczies J, Li Q, et al. An online survival analysis tool to rapidly assess the effect of 22,277 genes on breast cancer prognosis using microarray data of 1,809 patients. Breast cancer research and treatment. 2010/10/01 2010;123(3):725–31. [PubMed: 20020197]
38. Lánczky A, Nagy Á, Bottai G, Munkácsy G, Szabó A, Santarpia L, et al. miRpower: a web-tool to validate survival-associated miRNAs utilizing expression data from 2178 breast cancer patients. Breast cancer research and treatment. 2016/12/01 2016;160(3):439–46. [PubMed: 27744485]
39. Győrffy B, Schäfer R. Meta-analysis of gene expression profiles related to relapse-free survival in 1,079 breast cancer patients. Breast cancer research and treatment. 2009/12/01 2009;118(3):433–41. [PubMed: 19052860]
40. Győrffy B, Bottai G, Lehmann-Che J, Kéri G, Őrfi L, Iwamoto T, et al. TP53 mutation-correlated genes predict the risk of tumor relapse and identify MPS1 as a potential therapeutic kinase in TP53-mutated breast cancers. 2014;8(3):508–19.
41. Mihály Z, Kormos M, Lánczky A, Dank M, Budczies J, Szász MA, et al. A meta-analysis of gene expression-based biomarkers predicting outcome after tamoxifen treatment in breast cancer. Breast cancer research and treatment. 2013/07/01 2013;140(2):219–32. [PubMed: 23836010]
42. Győrffy B, Benke Z, Lánczky A, Balázs B, Szállási Z, Timár J, et al. RecurrenceOnline: an online analysis tool to determine breast cancer recurrence and hormone receptor status using microarray data. Breast cancer research and treatment. 2012/04/01 2012;132(3):1025–34. [PubMed: 21773767]
43. Li Q, Birkbak NJ, Gyorffy B, Szallasi Z, Eklund AC. Jetset: selecting the optimal microarray probe set to represent a gene. BMC Bioinformatics. 2011/12/15 2011;12(1):474. [PubMed: 22172014]
44. Ma XJ, Dahiya S, Richardson E, Erlander M, Sgroi DC. Gene expression profiling of the tumor microenvironment during breast cancer progression. Breast cancer research : BCR. 2009;11(1):R7. Epub 2009/02/04. [PubMed: 19187537]
45. Colak D, Nofal A, Albakheet A, Nirmal M, Jeprel H, Eldali A, et al. Age-specific gene expression signatures for breast tumors and cross-species conserved potential cancer progression markers in young women. PloS one. 2013;8(5):e63204–e. [PubMed: 23704896]
46. Borowsky AD, Namba R, Young LJ, Hunter KW, Hodgson JG, Tepper CG, et al. Syngeneic mouse mammary carcinoma cell lines: two closely related cell lines with divergent metastatic behavior. Clin Exp Metastasis. 2005;22(1):47–59. Epub 2005/09/01. [PubMed: 16132578]
47. Barkan D, Kleinman H, Simmons JL, Asmussen H, Kamaraju AK, Hoenorhoff MJ, et al. Inhibition of metastatic outgrowth from single dormant tumor cells by targeting the cytoskeleton. Cancer Res. Aug 1 2008;68(15):6241–50. Epub 2008/08/05. [PubMed: 18676848]
48. Boulanger MJ, Chow DC, Brevnova EE, Garcia KC. Hexameric structure and assembly of the interleukin-6/IL-6 alpha-receptor/gp130 complex. Science (New York, NY). Jun 27 2003;300(5628):2101–4. Epub 2003/06/28.

49. Taga T, Kishimoto T. Gp130 and the interleukin-6 family of cytokines. Annu Rev Immunol. 1997;15:797–819. Epub 1997/01/01. [PubMed: 9143707]
50. Yin T, Taga T, Tsang ML, Yasukawa K, Kishimoto T, Yang YC. Involvement of IL-6 signal transducer gp130 in IL-11-mediated signal transduction. The Journal of Immunology. 1993;151(5):2555. [PubMed: 8360477]
51. West NR. Coordination of Immune-Stroma Crosstalk by IL-6 Family Cytokines. Review 2019-May-15 2019;10(1093).
52. Mosley B, De Imus C, Friend D, Boiani N, Thoma B, Park LS, et al. Dual oncostatin M (OSM) receptors. Cloning and characterization of an alternative signaling subunit conferring OSM-specific receptor activation. J Biol Chem. Dec 20 1996;271(51):32635–43. Epub 1996/12/20. [PubMed: 8999038]
53. West NR, Murphy LC, Watson PH. Oncostatin M suppresses oestrogen receptor-α expression and is associated with poor outcome in human breast cancer. Endocrine-related cancer. Apr 2012;19(2):181–95. Epub 2012/01/24. [PubMed: 22267707]
54. Schröder J, Fietz T, Köhler A, Petersen V, Tesch H, Spring L, et al. Treatment and pattern of bone metastases in 1094 patients with advanced breast cancer – Results from the prospective German Tumour Registry Breast Cancer cohort study. European Journal of Cancer. 2017;79:139–48. [PubMed: 28494404]
55. Wang Z, Yang B, Zhang M, Guo W, Wu Z, Wang Y, et al. lncRNA Epigenetic Landscape Analysis Identifies EPIC1 as an Oncogenic lncRNA that Interacts with MYC and Promotes Cell-Cycle Progression in Cancer. Cancer Cell. 2018;33(4):706–20.e9. [PubMed: 29622465]
56. Bjorge J, Andy P, Funnell M, Chen K, Diaz R, Magliocco A, et al. Simultaneous siRNA Targeting of Src and Downstream Signaling Molecules Inhibit Tumor Formation and Metastasis of a Human Model Breast Cancer Cell Line. PloS one. 04/26 2011;6:e19309. [PubMed: 21541295]
57. Chiu J-H, Wen C-S, Wang J-Y, Hsu C-Y, Tsai Y-F, Hung S-C, et al. Role of estrogen receptors and Src signaling in mechanisms of bone metastasis by estrogen receptor positive breast cancers. Journal of translational medicine. 2017;15(1):97-. [PubMed: 28472954]
58. Defilippi P, Di Stefano P, Cabodi S. p130Cas: a versatile scaffold in signaling networks. Trends in cell biology. May 2006;16(5):257–63. Epub 2006/04/04. [PubMed: 16581250]
59. Finn RS. Targeting Src in breast cancer. Annals of Oncology. 2008/08/01/ 2008;19(8):1379–86. [PubMed: 18487549]
60. Campbell JP, Merkel AR, Masood-Campbell SK, Elefteriou F, Sterling JA. Models of bone metastasis. Journal of visualized experiments : JoVE. Sep 4 2012(67):e4260. Epub 2012/09/14. [PubMed: 22972196]
61. Jorcyk CL, Holzer RG, Ryan RE. Oncostatin M induces cell detachment and enhances the metastatic capacity of T-47D human breast carcinoma cells. Cytokine. 2006/03/21/ 2006;33(6):323–36. [PubMed: 16713283]
62. West NR, Murray JI, Watson PH. Oncostatin-M promotes phenotypic changes associated with mesenchymal and stem cell-like differentiation in breast cancer. Oncogene. Mar 20 2014;33(12):1485–94. Epub 2013/04/16. [PubMed: 23584474]
63. Bolin C, Tawara K, Sutherland C, Redshaw J, Aranda P, Moselhy J, et al. Oncostatin M Promotes Mammary Tumor Metastasis to Bone and Osteolytic Bone Degradation. Genes & Cancer. 2012;3(2):117–30. [PubMed: 23050044]
64. Chong YP, Ia KK, Mulhern TD, Cheng HC. Endogenous and synthetic inhibitors of the Src-family protein tyrosine kinases. Biochimica et biophysica acta. Dec 30 2005;1754(1–2):210–20. Epub 2005/10/04. [PubMed: 16198159]
65. Xu W, Doshi A, Lei M, Eck MJ, Harrison SC. Crystal structures of c-Src reveal features of its autoinhibitory mechanism. Molecular cell. May 1999;3(5):629–38. Epub 1999/06/09. [PubMed: 10360179]
66. Cowan-Jacob SW, Fendrich G, Manley PW, Jahnke W, Fabbro D, Liebetanz J, et al. The crystal structure of a c-Src complex in an active conformation suggests possible steps in c-Src activation. Structure (London, England : 1993). Jun 2005;13(6):861–71. Epub 2005/06/09.

67. Myoui A, Nishimura R, Williams PJ, Hiraga T, Tamura D, Michigami T, et al. C-Src Tyrosine Kinase Activity Is Associated with Tumor Colonization in Bone and Lung in an Animal Model of Human Breast Cancer Metastasis. Cancer Research. 2003;63(16):5028. [PubMed: 12941830]

68. Kanomata N, Kurebayashi J, Kozuka Y, Sonoo H, Moriya T. Clinicopathological significance of Y416Src and Y527Src expression in breast cancer. Journal of clinical pathology. Jul 2011;64(7):578–86. Epub 2011/04/15. [PubMed: 21490376]

69. Zhang L, Teng Y, Zhang Y, Liu J, Xu L, Qu J, et al. c-Src expression is predictive of poor prognosis in breast cancer patients with bone metastasis, but not in patients with visceral metastasis. APMIS : acta pathologica, microbiologica, et immunologica Scandinavica. Jul 2012;120(7):549–57. Epub 2012/06/22.

70. Tawara K, Bolin C, Koncinsky J, Kadaba S, Covert H, Sutherland C, et al. OSM potentiates preintravasation events, increases CTC counts, and promotes breast cancer metastasis to the lung. Breast cancer research : BCR. Jun 14 2018;20(1):53. [PubMed: 29898744]

71. Sleeman MW, Anderson KD, Lambert PD, Yancopoulos GD, Wiegand SJ. The ciliary neurotrophic factor and its receptor, CNTFRα. Pharmaceutica acta Helvetiae. 2000/03/01/ 2000;74(2):265–72. [PubMed: 10812968]

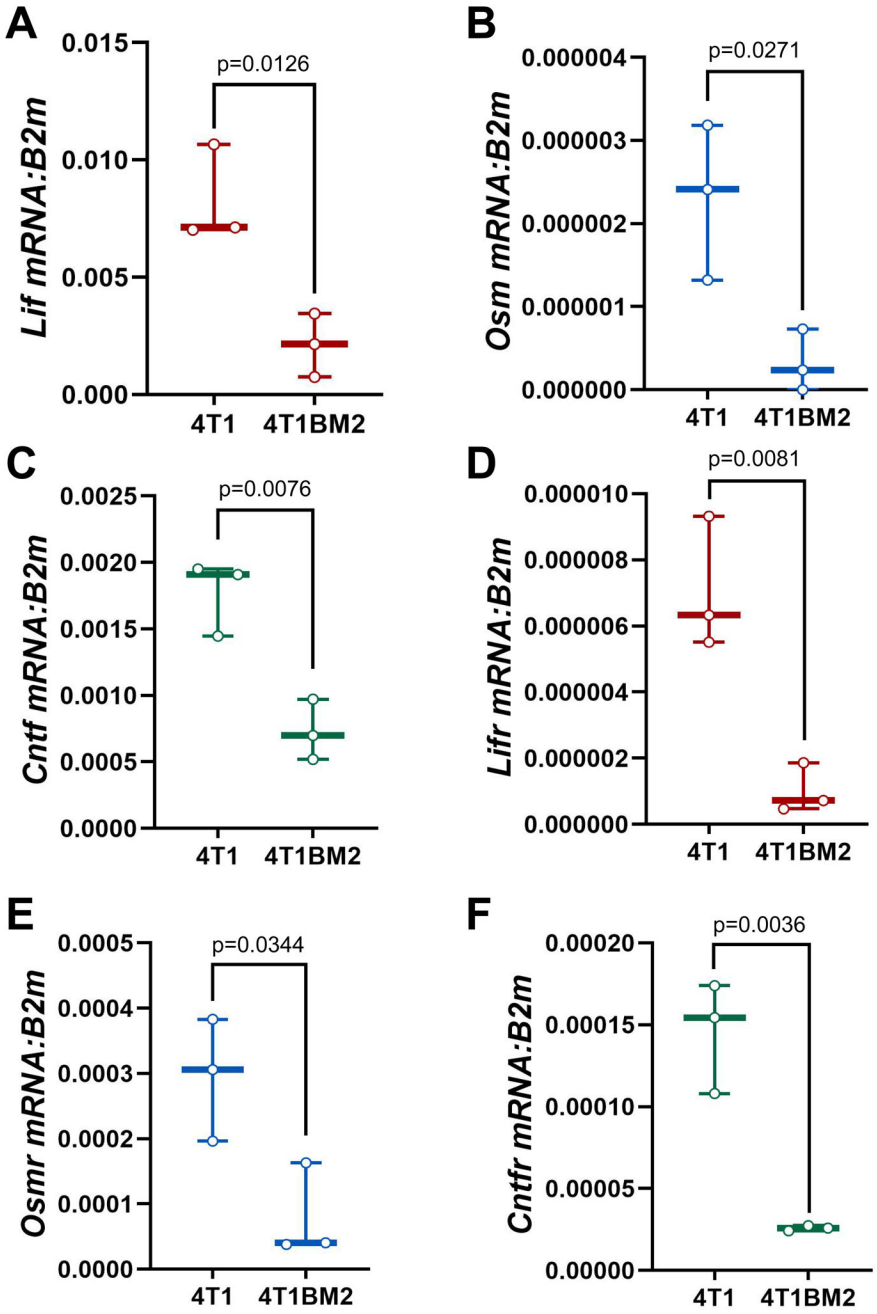

Figure 1. Comparison of the relative expression of the gp130 ligands in parental and bone metastatic variants of 4T1 breast cancer cell lines.

(A-F) qPCR analysis of parental 4T1 and 4T1BM2 cells (bone metastatic) (A) *Lif*, (B) *Osm*, (C) *Cntf*, (D) *Lifr*, (E) *Osmr*, and (F) *Cntfr* mRNA levels normalized to *B2M* (housekeeping gene). Student's unpaired t-test. n=three independent biological replicates. Boxplots represent mean + interquartile range.

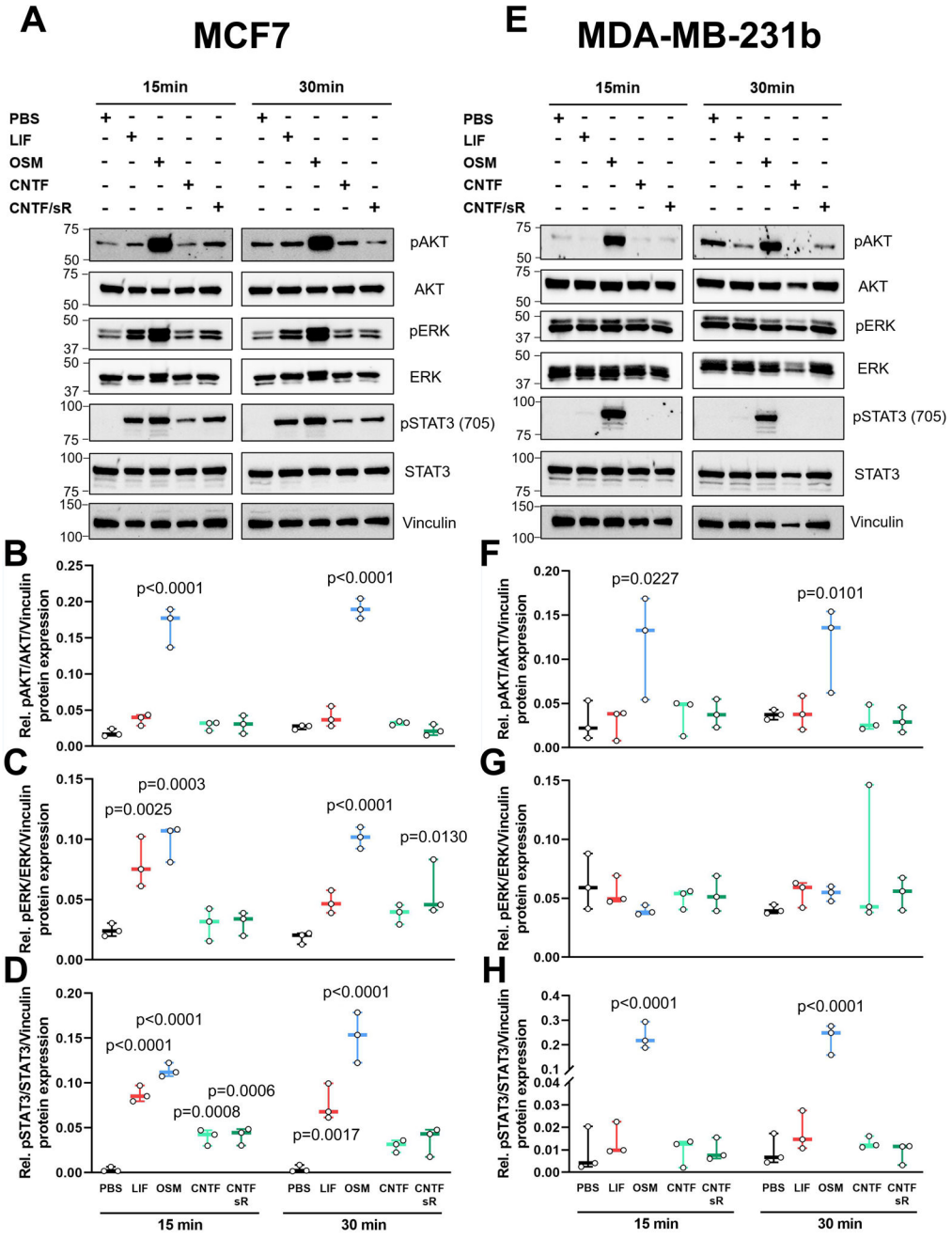

Figure 2. LIFR-binding ligands activate AKT, ERK, and STAT3 signaling pathways in MCF7 and MDA-MB-231 cells.

(A-H) Western blot analysis for pAKT^{S473}, total AKT, pERK$^{T202–204}$, total ERK, pSTAT3^{Y705}, total STAT3 and vinculin (loading control) after 15 or 30 minute treatment with PBS, recombinant LIF, recombinant OSM, recombinant CNTF at 50 ng mL^{-1} and a 1:10 ratio of CNTF and its soluble receptor CNTF (50:500 μg mL^{-1}) in (A-D) MCF7 and (E-H) MDA-MB-231b breast cancer cells. (A, E) Representative western blot images for MCF7 and MDA-MB-231b cells treated with the respective cytokines. (B-D, F-H) Densitometry analysis from western blot images developed from 3 biological replicates of MCF7 and MDA-MB-231b cells treated with the respective cytokines. One-way ANOVA

with Sidak's multiple comparisons. n=three independent biological replicates. Boxplots represent mean + interquartile range.

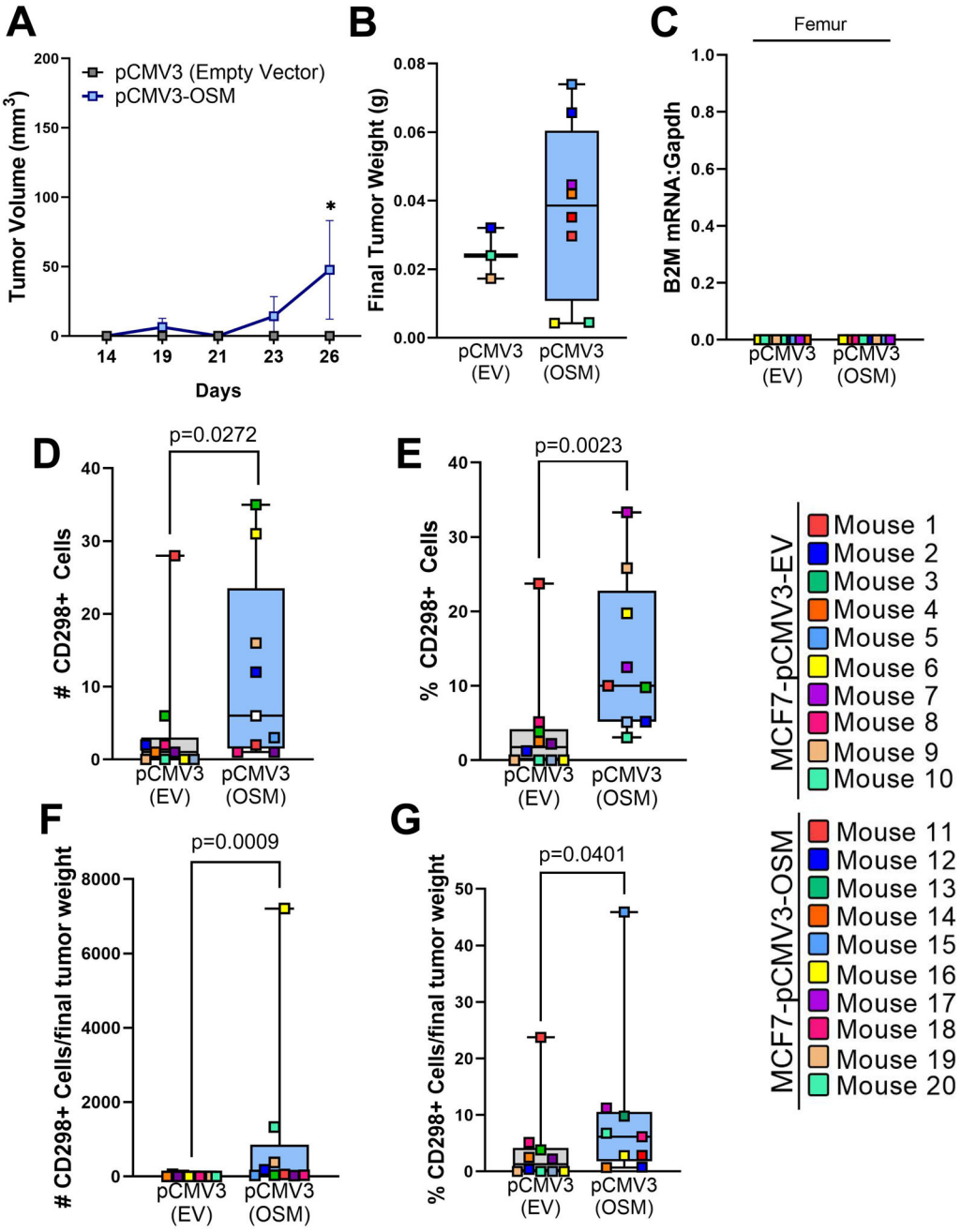

Figure 3. Overexpression of OSM promotes spontaneous dissemination of MCF7 cells to the bone.

(A-G) *In vivo* analysis of MCF7 OSM/CNTF overexpressing cells. n=10 mice/group for MCF7-pCMV3, n=9 mice/group for MCF7-pCMV3-OSM. (A) Tumor volume by caliper measurements over 26 days following injection of MCF7-pCMV3 (empty vector), MCF7-pCMV3-OSM (OSM over-expression). (B) Final tumor weight after sacrifice. (C) qPCR analysis of *B2M* expression in homogenized femur from inoculated mice normalized to mouse *Gapdh* (housekeeping gene). (D, E) Quantification of the total number (D) and percentage (E) of CD298+ tumor cells detected by flow cytometry in the bone marrow of inoculated mice. (F, G) Normalization of total number (F) and percentage (G) of CD298+

cells to final tumor weight. A: Two-way ANOVA with Tukey's multiple comparisons test. B-G: Mann-Whitney Test. n=three independent biological replicates. Boxplots represent mean + interquartile range.

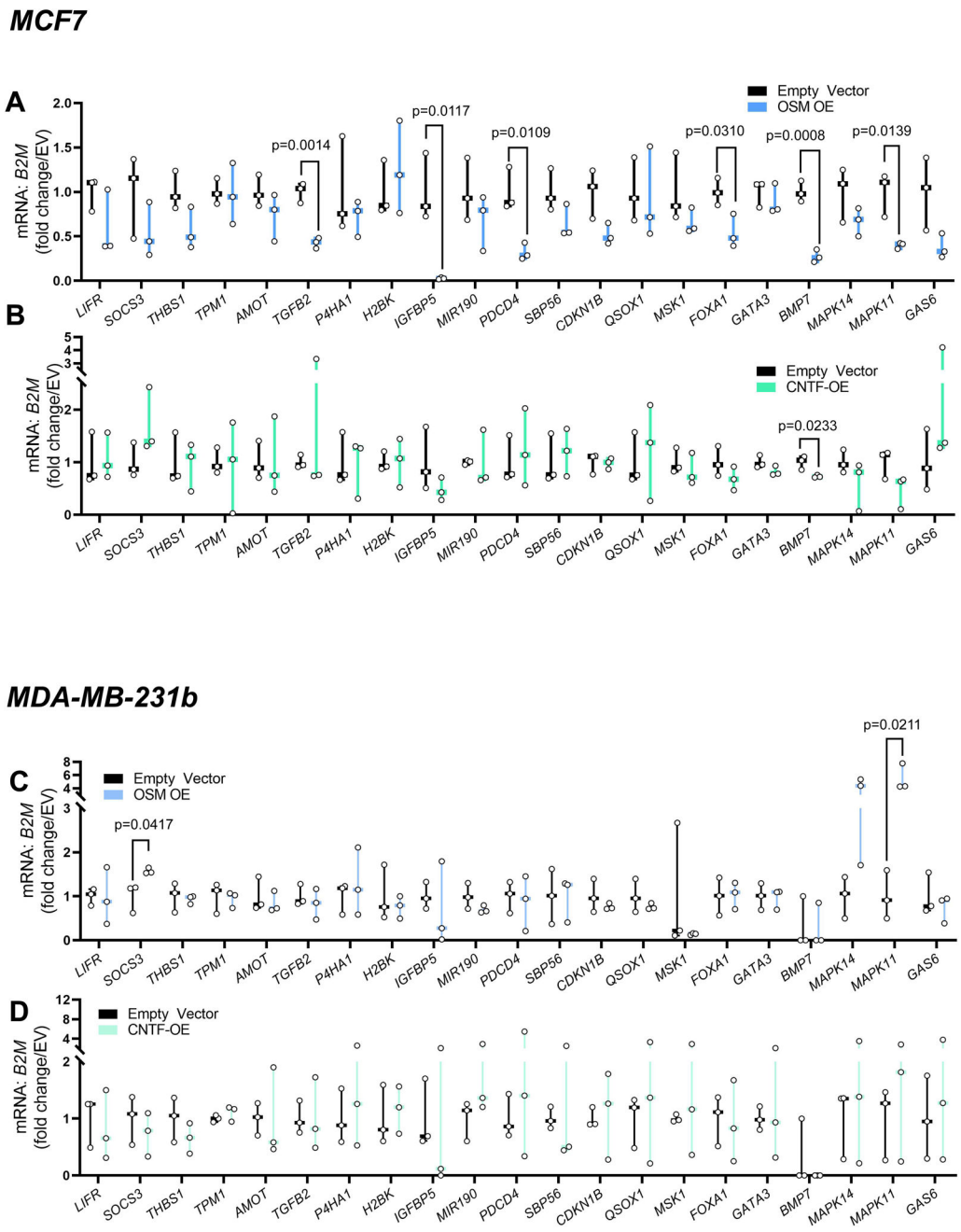

Figure 4. Overexpression of OSM downregulates the expression of several dormancy genes in MCF7 but not MDA-MB-231b breast cancer cells.

(A, B) MCF7 cells with constitutive expression of OSM or CNTF were assessed for mRNA expression levels of genes associated with dormancy. (C, D) MDA-MB-231b cells with transient expression of OSM or CNTF were assessed for mRNA expression levels of genes associated with dormancy. n=3 independent biological replicates. A-H: Student's unpaired t-test. n=three independent biological replicates. Boxplots represent mean + interquartile range.

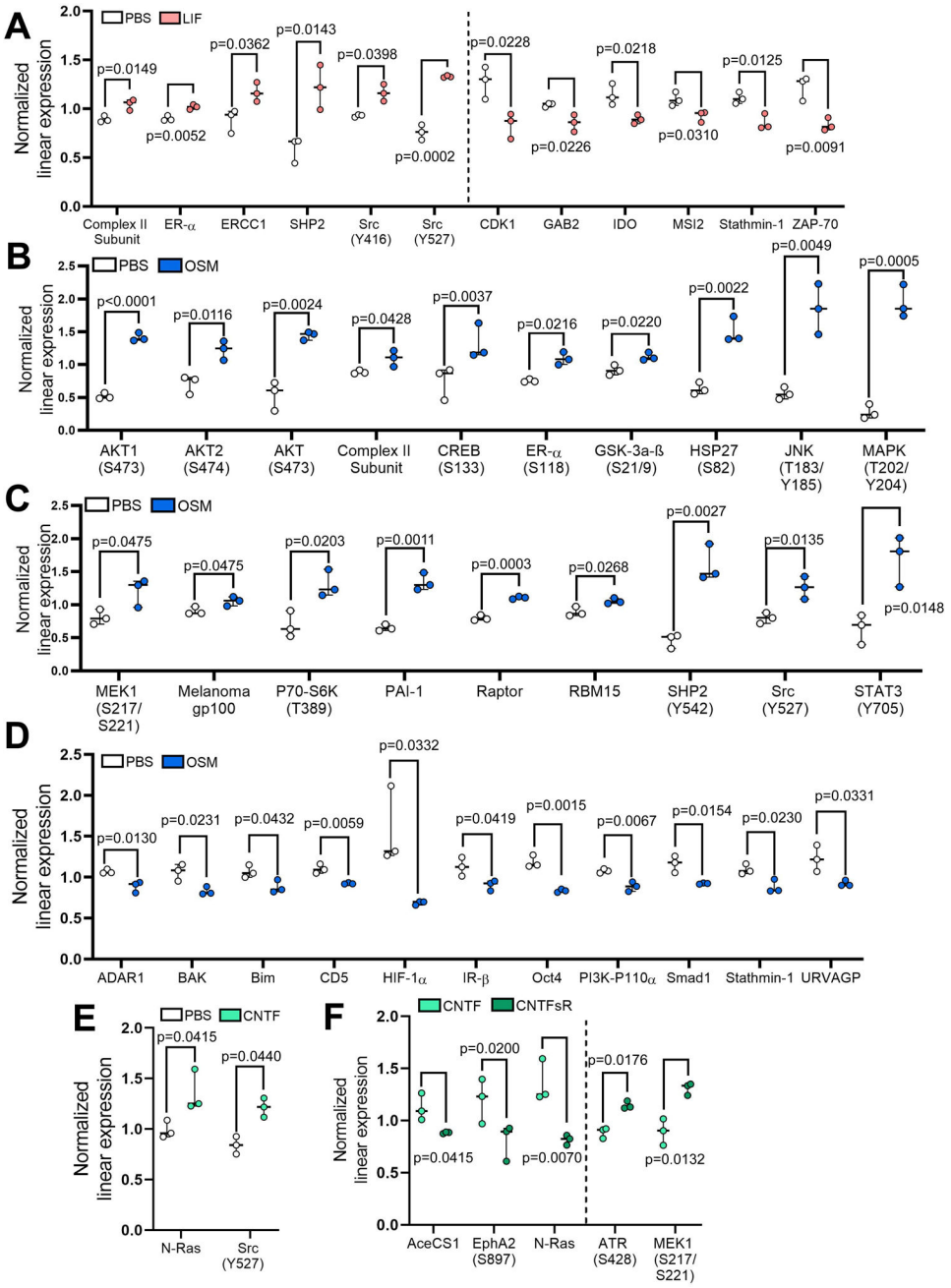

Figure 5. The gp130 cytokines activate multiple signaling pathways in breast cancer cells.

(A-E) Proteins significantly altered by the gp130 cytokine family evaluated by RPPA in MCF7 cells treated for 30 minutes with PBS, recombinant LIF, recombinant OSM, recombinant CNTF at 50 ng mL^{-1} and a 1:10 ratio of CNTF and its soluble receptor CNTF (50:500 μg mL^{-1}). Normalized linear protein expression of the significantly regulated proteins by (A) *LIF*, (B,C,D) *OSM*, (E) *CNTF*, and (F) *CNTFsR* treatment. One-way ANOVA with Sidak's multiple comparisons test. n=three independent biological replicates. Boxplots represent mean + interquartile range.

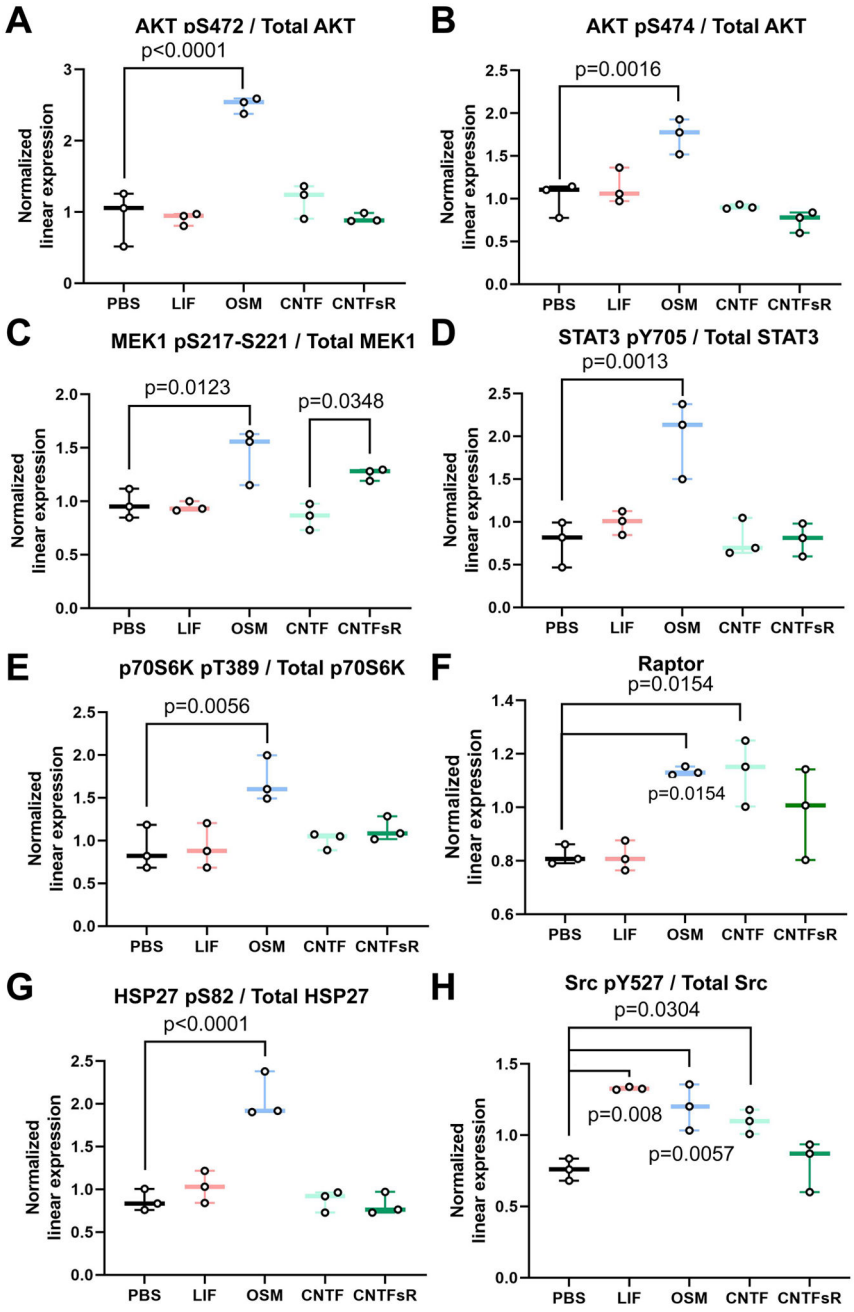

Figure 6. OSM activates several downstream signaling pathways in breast cancer cells.

(A-H) Normalized linear protein expression of the significantly regulated proteins in MCF7 cells by OSM. (A) AKT (p<0.0001), (B) AKT2 (p=0.0016), (C) MEK1 (p=0.0123), (D) STAT3 (p=0.0013), (E) p70-S6K (p=0.0056), (F) Raptor (p=0.0154), (G) HSP27 (p<0.0001), and (H) Src (p=0.0057) were all significantly upregulated by OSM treatment. One-way ANOVA with Sidak's multiple comparisons test. n=three independent biological replicates. Boxplots represent mean + interquartile range.

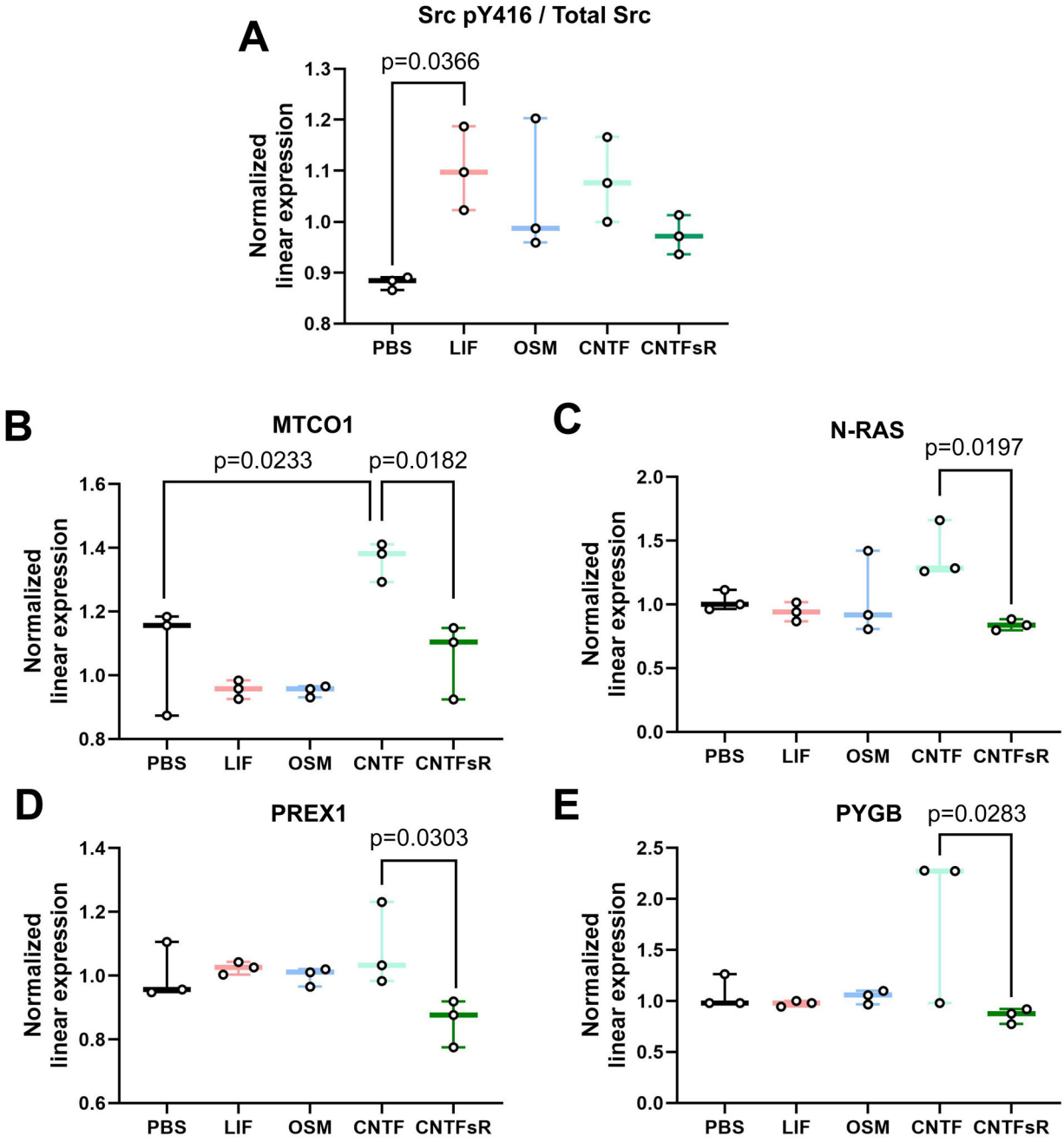

Figure 7. LIF activates Src^{Y416} and novel CNTF/CNTFsR signaling activates several previously unknown downstream effectors in breast cancer cells.

(A-E) Normalized linear protein expression of the significantly regulated proteins in MCF7 cells by LIF and CNTF/CNTFsR. (A) Src^{Y416} (p=0.0366) was the only protein upregulated by LIF alone. (B) MTCO1 (p=0.0233), (C) N-Ras (p=0.0197), (D) PREX1 (p=0.0303), and (E) PYGB (p=0.0283) were significantly downregulated by CNTFsR signaling. One-way ANOVA with Sidak's multiple comparisons test. n=three independent biological replicates. Boxplots represent mean + interquartile range.

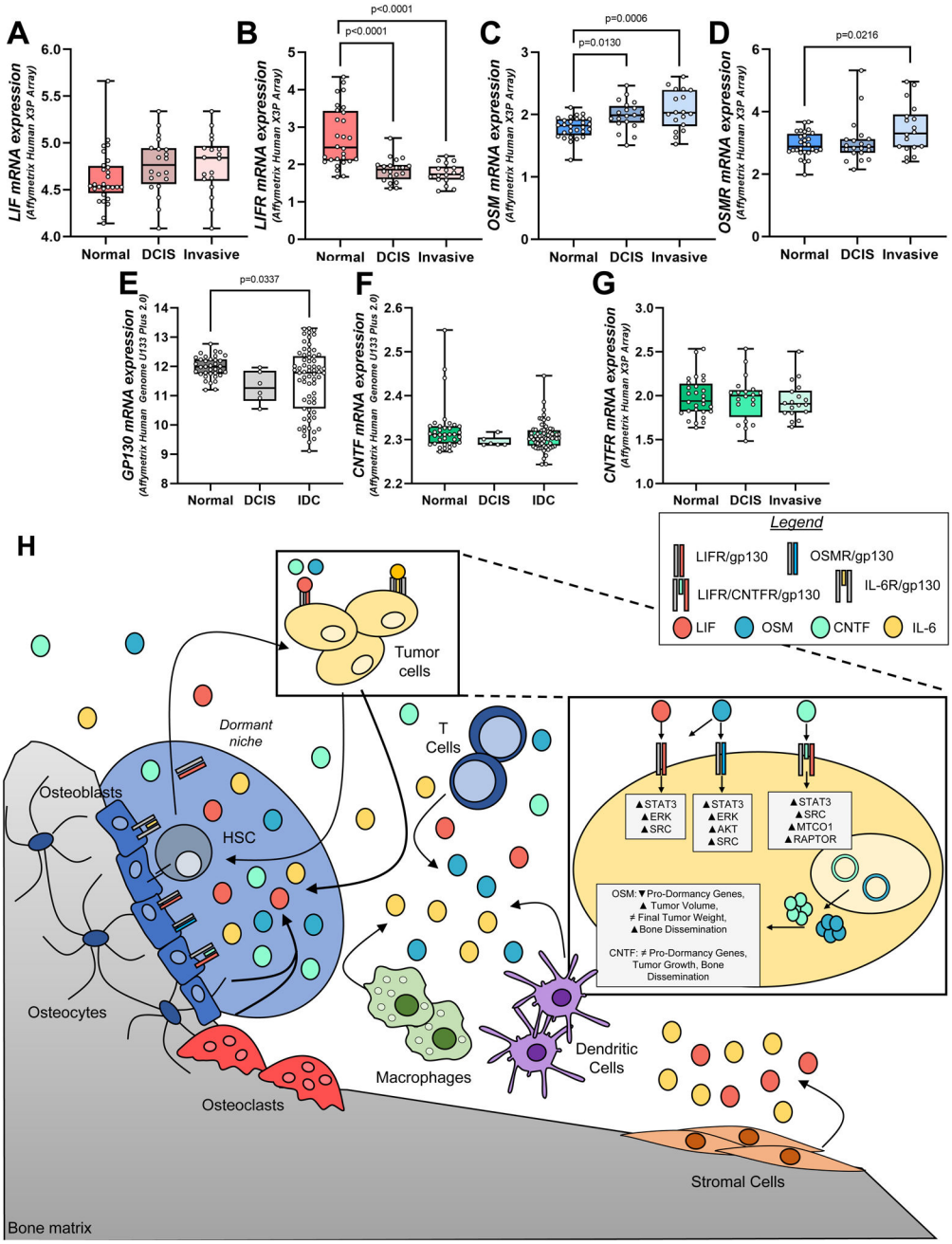

Figure 8. Differential expression of the gp130 cytokines and receptors in clinical patient data sets.

(A-G) LIF, LIFR, OSM, OSMR, GP130, CNTF and CNTFR mRNA expression in normal, ductal carcinoma in situ (DCIS) and invasive ductal carcinoma (IDC) patient samples from GSE14548 (A, B, C, D, F, G) and GSE29044 (E). A-G: One-way ANOVA with Sidak's multiple comparisons test. GSE14548: n= (Normal: 28, DCIS: 20, Invasive: 18). GSE29044: n= (Normal: 36, DCIS: 6, IDC: 67). n=three independent biological replicates. Boxplots represent mean + interquartile range. (H) Tumor cells that metastasize and colonize the bone marrow, invade and establish within the endosteal niche resulting in increased interaction with dormant hematopoietic stem cells (HSCs). Our group and other propose that these

tumor cells outcompete HSCs for important self-renewal and dormancy-related factors pertinent for HSC maintenance and survival. In conjunction, gp130 cytokines are expressed and produced by hemotopoietic lineage cells, osteoblast lineage cells, and stromal cells, suggesting that tumor cells encounter the cytokines via paracrine cytokine signaling. These signals then activate STAT3, ERK, AKT, and Src signaling, among other cytokine-specific pathways, to regulate tumor progression and bone dissemination.